Dynamic profiling of mRNA turnover reveals gene-specific and system-wide regulation of mRNA decay

Sarah E. Munchel*, Ryan K. Shultzaberger[†], Naoki Takizawa, and Karsten Weis
Department of Molecular and Cellular Biology and QB3, University of California, Berkeley, Berkeley, CA 94720

ABSTRACT RNA levels are determined by the rates of both transcription and decay, and a mechanistic understanding of the complex networks regulating gene expression requires methods that allow dynamic measurements of transcription and decay in living cells with minimal perturbation. Here, we describe a metabolic pulse-chase labeling protocol using 4-thiouracil combined with large-scale RNA sequencing to determine decay rates of all mRNAs in *Saccharomyces cerevisiae*. Profiling in various growth and stress conditions reveals that mRNA turnover is highly regulated both for specific groups of transcripts and at the system-wide level. For example, acute glucose starvation induces global mRNA stabilization but increases the degradation of all 132 detected ribosomal protein mRNAs. This effect is transient and can be mimicked by inhibiting the target-of-rapamycin kinase. Half-lives of mRNAs critical for galactose (GAL) metabolism are also highly sensitive to changes in carbon source. The fast reduction of *GAL* transcripts in glucose requires their dramatically enhanced turnover, highlighting the importance of mRNA decay in the control of gene expression. The approach described here provides a general platform for the global analysis of mRNA turnover and transcription and can be applied to dissect gene expression programs in a wide range of organisms and conditions.

INTRODUCTION

Rapid and precise changes in gene expression are essential for all aspects of cellular physiology, and eukaryotic cells effectively regulate their gene expression programs by rapidly adjusting their transcriptome. Transcript abundance is determined by a balance of mRNA production and degradation, but the speed by which cells can adjust their mRNA levels is critically dependent on the rate of

mRNA turnover. Although the regulation of transcriptional control has been studied extensively, little is known about how mRNA turnover is regulated and the degree to which transcriptome-wide changes depend on transcript degradation. To dissect the regulatory networks that control gene expression and better understand the kinetics of the cellular response, it is critical not only to examine transcriptional changes, but also to identify the principles that govern the system-wide regulation of mRNA turnover.

In eukaryotes, the bulk of mRNA decay occurs in a deadenylation-dependent manner. Following removal of the poly(A) tail, mRNA is degraded in either a 5′–3′ or 3′–5′ direction (Coller and Parker, 2004; Garneau *et al.*, 2007). Degradation from the 3′–5′ direction is carried out by a large, multisubunit complex of 3′-to-5′ exonucleases called the exosome. Alternatively, in the 5′–3′ degradation pathway, the m7G mRNA cap is cleaved first by the Dcp1/Dcp2 decapping complex and the monophosphate RNA is degraded progressively by the 5′–3′ exonuclease Xrn1 (Coller and Parker, 2004; Garneau *et al.*, 2007).

Of interest, many components of the mRNA degradation machinery are specifically localized in the cytoplasm to distinct, non–membrane-bound foci called processing bodies (P bodies; Parker and Sheth, 2007). Proteins involved in both the 5′–3′ and

3′–5′ degradation pathways localize to these structures. Furthermore, mRNAs targeted for decay are detected in P bodies upon inhibition of mRNA turnover, suggesting a function of P bodies in mRNA degradation (Eulalio *et al.*, 2007; Parker and Sheth, 2007). P body–like structures have been identified in many eukaryotes, indicating that their function is evolutionarily conserved (Eulalio *et al.*, 2007). In budding yeast, P bodies are apparent only in response to stress, and the number of P bodies rises when the cellular pool of nontranslating mRNAs increases (Eulalio *et al.*, 2007; Parker and Sheth, 2007; Franks and Lykke-Andersen, 2008). The significant increase of P bodies in response to stress indicates that mRNA decay and translational inhibition play an important role in the cellular stress response.

Although the general mechanism of mRNA degradation has been well studied, it remains unclear how cells regulate changes systemically or for individual transcripts. Microarray analyses have suggested that up to 50% of changes in gene expression in response to cellular signals can occur at the level of mRNA stability (Cheadle *et al.*, 2005). To understand mRNA turnover at a genome-wide level, several studies have looked at global patterns in turnover by directly measuring mRNA decay rates upon inhibition of transcription (Wang *et al.*, 2002; Grigull *et al.*, 2004; Sharova *et al.*, 2009). However, transcriptional inhibition blocks growth and has a profound effect on cellular physiology, as well as on mRNA metabolism (Pelechano and Perez-Ortin, 2008). Furthermore, these studies were unable to perform mRNA half-life measurements in response to changing conditions or in response to cellular stress.

To measure global changes in mRNA turnover, we developed a pulse-chase RNA labeling protocol in *Saccharomyces cerevisiae*, which enabled us to directly measure endogenous mRNA decay rates (Figure 1A). Our in vivo labeling system does not perturb the cell and allows for a wide variety of conditions to be monitored. Combined with quantitative RNA deep sequencing technology (RNA-seq; Wang *et al.*, 2009; Wilhelm and Landry, 2009), we were able to measure the dynamics of mRNA turnover on a genome-wide scale under a variety of physiological or stress conditions.

RESULTS AND DISCUSSION
mRNA turnover during logarithmic growth in glucose
To develop a noninvasive method to determine system-wide mRNA turnover rates, we took advantage of sulfur-substituted nucleotide precursors, which can be used to biosynthetically label newly synthesized RNAs in vivo (Cleary *et al.*, 2005; Wilhelm and Landry, 2009). 4-Thiouracil (4TU) is rapidly taken up by *S. cerevisiae* and converted into UTP for incorporation into all classes of RNA with no detectable effects on cellular growth or physiology (Figure 1B, Supplemental Figure S1a and unpublished data). It is important that 4TU incorporation can easily be quenched in the presence of high uracil concentrations (Figure 1C), making this an ideal label for pulse-chase experiments to monitor mRNA turnover. To measure decay rates, yeast cultures were grown in the presence of 0. 2 mM 4TU for two generations and then shifted into media that lacked 4TU but contained 20 mM uracil. mRNA was isolated for at least five time points during a 60-min time course, and thio-labeled RNA was modified with a thio-reactive biotinylation reagent, which allowed for selective purification of labeled RNA via streptavidin beads (Supplemental Figure S1b).

We first used this approach to determine mRNA decay rates during optimal growth conditions in synthetic medium containing 2% glucose. Two independent time courses were analyzed by quantitative RNA-seq, yielding 7–14.5 million sequence reads for each time point. Reads were mapped to all *S. cerevisiae* open reading frame

sequences, including introns, using Bowtie (Langmead *et al.*, 2009), normalized to a spiked-in control RNA, and a single-exponential decay curve was fitted to the data from each mapped mRNA to determine individual half-lives. To ensure that the half-life calculation was not biased by an incomplete chase of the 4TU, the 0-min time point was omitted from the analysis. Data for 93% of the genes could be fitted by a single exponential decay curve with $R^2 \geq 0.8$, with an average R^2 for all genes of 0.95 (Figure 1D). This suggests that our chase protocol is efficient and that the majority of mRNAs in yeast are degraded with a first-order decay rate.

Results generated by this approach are highly reproducible between biological replicates. An excellent correlation was observed between two independent data sets with r values of 0.98, 0.98, 0.99, and 0.99 for the relative numbers of reads at increasing time points (Figure 2). Despite this very high correlation between experiments, the correlation for the calculated half-lives was lower (R = 0.7). This lower correlation is most likely due the relatively limited number of time points that were collected for the half-life determination. This, in combination with small discrepancies in measurements between time points and small errors that are introduced by the normalization, will reduce the accuracy of the half-life calculation. The high reproducibility of our measurements is illustrated by a set of 12 mRNAs that fit a single-exponential decay model with $R^2 = 1$ in the two experiments (Supplemental Figure S2). Comparing all mRNAs that have an $R^2 > 0.8$ for both experiments, we find that 77% of mRNAs varied in their half-lives by 5 min or less and only 5% varied by 10 min or more, with an enrichment for long-lived mRNAs.

Using this method, we detected a wide distribution of mRNA half-lives. Figure 3A shows examples of individual curves for a range of turnover rates. The half-lives for all mRNAs with $r^2 > 0.8$ are reported in Supplemental Table S1, and individual decay curves for the complete data set are available online (http://rnadecay.berkeley .edu/). Global analysis of 5736 yeast mRNAs revealed an average half-life of 20.1 min with SD of 8.6 min and median half-life of 18 min (Figure 3B). This is consistent with data previously published by Wang *et al.* (2002), who reported an average half-life of 23 min with a median of 20 min. However, there was no overall correlation between our data set and individual half-life measurements obtained upon transcriptional inhibition R = 0 for the comparison between our data set and the results of Wang *et al.* (2002); Supplemental Figure S3]. Furthermore, there was no obvious correlation between mRNA half-life and transcript abundance, transcript length, or other mRNA features, including 5′ and 3′ untranslated region (UTR) length (unpublished data). Generally, we observed a tight distribution of decay rates: 91% of all mRNAs have a half-life between 12 and 29 min, falling within approximately one SD of the mean of the distribution (Figure 3B). Gene ontology analysis showed that transcripts with a half-life of 12 min or less were functionally enriched for "small molecule metabolic processes" ($p = 5e^{-30}$), including mRNAs for lysine ($p = 1e^{-7}$) and arginine ($p = 2e^{-3}$) biosynthesis genes. Transcripts with half-lives of greater than 28 min were functionally enriched for genes involved in RNA-mediated transposition ($p = 1e^{-50}$) and translation ($p = 7e^{-18}$).

One of the largest half-life groups therein comprises 132 mRNAs coding for ribosomal proteins of the large and small ribosomal particle with an average half-life of 38 min. It is intriguing that based on the use of transcriptional shut-off, the half-lives of these mRNAs have previously been reported to be significantly shorter (~20 min; Wang *et al.*, 2002), suggesting that inhibition of transcription may lead to destabilization of this group. Indeed, the turnover of mRNAs encoding ribosomal protein is increased during cellular stress and is highly dependent on growth conditions (see Figure 5 later in the paper).
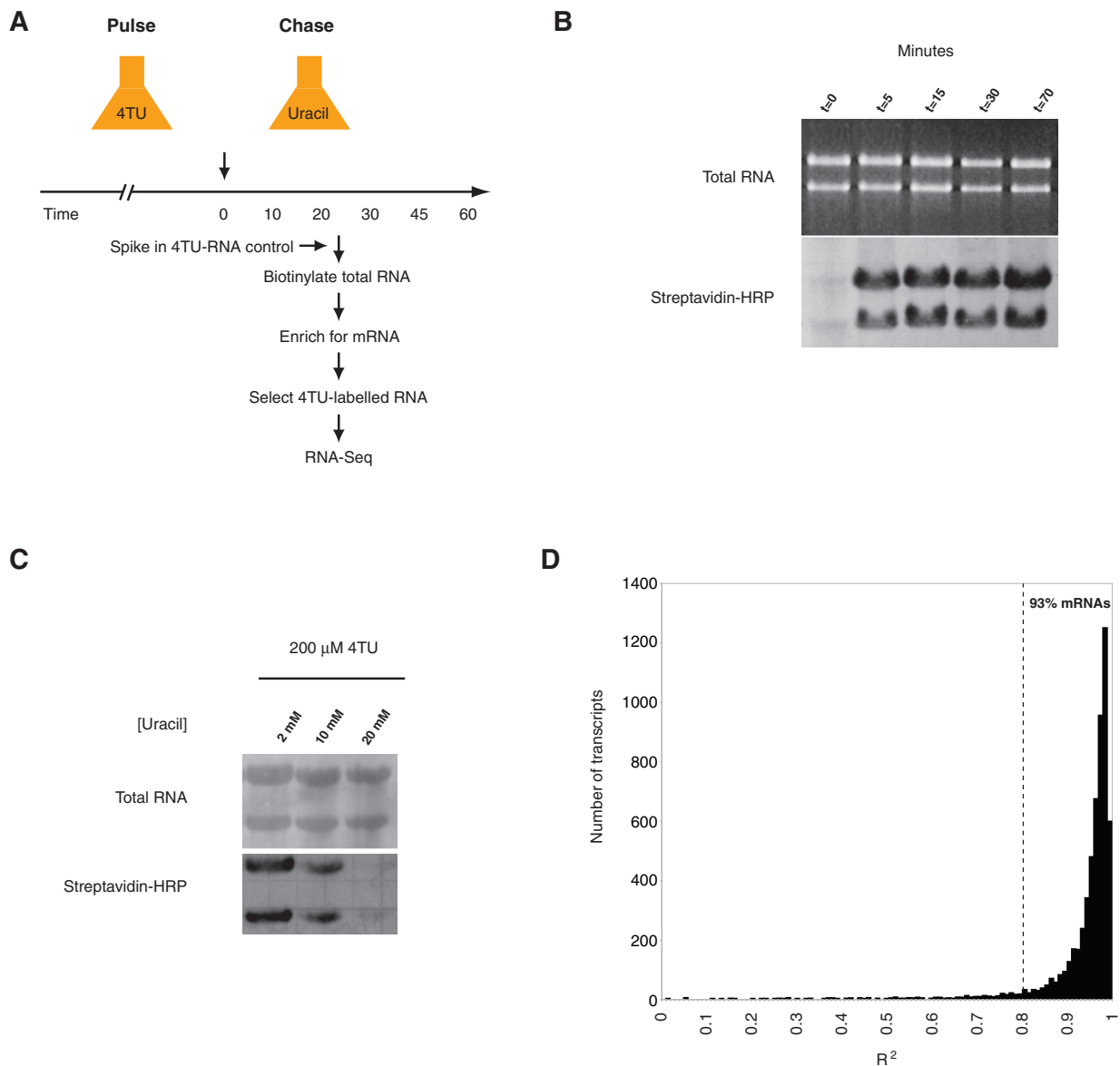
FIGURE 1: Pulse-chase methodology for measuring mRNA turnover. (A) Schematic of pulse-chase protocol for determining genome-wide mRNA half-lives. Cultures were grown in the presence of 0.2 mM 4TU and then shifted into medium containing 20 mM uracil. Total RNA was isolated at different times after the shift into the chase media. A constant amount of 4TU-containing control RNA was spiked in as a reference for analysis. Each sample was biotinylated, enriched for mRNA populations, and purified on streptavidin beads. Samples were then analyzed following standard RNA-seq protocols. For details see Supplemental Materials. (B) Sulfur-modified nucleotides are rapidly incorporated into RNA. *S. cerevisiae* cells were grown to midlog phase in minimal medium. At t = 0, 0.2 mM 4TU was added to the medium, and samples were collected at indicated time points. Total RNA was isolated, incubated with biotin-HPDP to label 4TU-modified RNA, and separated by gel. Total RNA was monitored by ethidium bromide staining and biotin was detected by streptavidin–horseradish peroxidase (HRP). (C) 4TU incorporation is completely suppressed in the presence of 20 mM uracil. Yeast cultures were grown in minimal medium with indicated concentrations of uracil and 4TU for two doublings. Total RNA was isolated and labeled with biotin-HPDP and separated by gel electrophoresis and transferred to a nitrocellulose membrane. Total RNA levels were monitored by methylene blue staining, and biotinylated population was detected by streptavidin-HRP. (D) Data for all time points for each transcript were fitted to a first-order exponential decay model, and the R^2 value was calculated. The distribution of the R^2 values for all mRNAs is shown.

mRNA decay profile in galactose

Having established a global decay profile in logarithmic growth conditions in glucose, we next looked at the effect of cellular growth on mRNA degradation and profiled mRNA turnover in the presence of the carbon source galactose. Growth in galactose causes a significant change in the metabolic profile of yeast, resulting in an increase in their doubling time from ~1.5 to 3 h (Lohr *et al.*, 1995; Zaman *et al.*, 2008). However, the overall distribution of half-lives measured in this condition was similar to the turnover profile generated for yeast grown in glucose, with an average half-life of 19.4 min (SD, 8.7 min; median, 17 min; Figure 4A). Furthermore, the two data sets were positively correlated (R = 0.55 for mRNAs that have $R^2 \geq 0.8$ for both data sets; Figure 4B), and comparison of several individual decay curves showed similar turnover rates (Supplemental Figure S4).
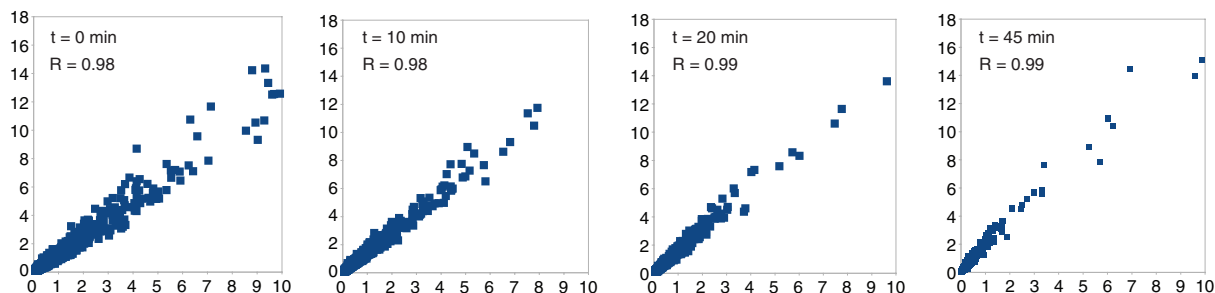
FIGURE 2: 4TU pulse chase is highly reproducible. Comparison of steady-state mRNA levels at individual time points for two independent biological replicates grown in dextrose. The *x*- and *y*-axes indicate number of transcripts ×10⁴. The R values are indicated for each time point.

Thus, the increased doubling time upon growth in galactose compared with glucose is not mirrored by a global decrease in mRNA turnover.

Interesting exceptions include mRNAs encoding for RNA-mediated transposition factors, which showed a significant shift in their half-lives in galactose versus glucose. The average half-life of the 95 RNAs annotated to function in RNA-mediated transposition in glucose is 34 min, whereas their average half-life in galactose is 24 min. Of the 50 genes that have the largest absolute difference in half-lives between the galactose and glucose data sets, 7 function in RNA-mediated transposition including mRNAs of the Ty1 class of retrotransposons (p = 2e⁻⁸; Figure 3C and Supplemental Tables S2 and S3). No obvious correlation between mRNA stability and expression levels or transcript length could be detected. Furthermore, we were unable to identify any specific sequence motifs that were enriched in mRNAs that displayed a shortening mRNA half-life upon growth in galactose. The physiological relevance of the Ty mRNA half-life change in galactose for retrotransposition remains unclear. Ty retrotransposition in yeast is a rare event despite the fact that Ty mRNAs, such as Ty1 mRNA, are highly expressed. It is intriguing that

Ty1 retrotransposition is significantly increased when Ty1 mRNA is expressed from a galactose-inducible galactose (GAL) promoter (Boeke *et al.*, 1985). Furthermore, it was recently shown that several components of the 5′–3′ decay machinery are required for efficient retrotransposition. However, the mechanistic role of the decay machinery in retrotransposition remains unclear (Checkley *et al.*, 2010; Dutko *et al.*, 2010), and further experiments will be necessary to understand whether the change in half-life that we observe here has a consequence on the efficiency of retrotransposition.

Monitoring mRNA turnover upon acute carbon source change from galactose to glucose

When grown in galactose, yeast cells highly induce the expression of several genes critical for galactose fermentation, including *GAL1*, *2*, *3*, *5*, *7*, and *10* (Lohr *et al.*, 1995). In galactose, the average half-life of these induced *GAL* mRNAs is 18 min (Table 1). Of interest, much shorter half-lives have been previously reported upon transcriptional inhibition by the addition of glucose [e.g., *GAL1* $t_{1/2}$ = 4 min and GAL3 $t_{1/2}$ = 3 min (Bennett *et al.*, 2008)]. A principal advantage of our pulse-chase method is the ability to
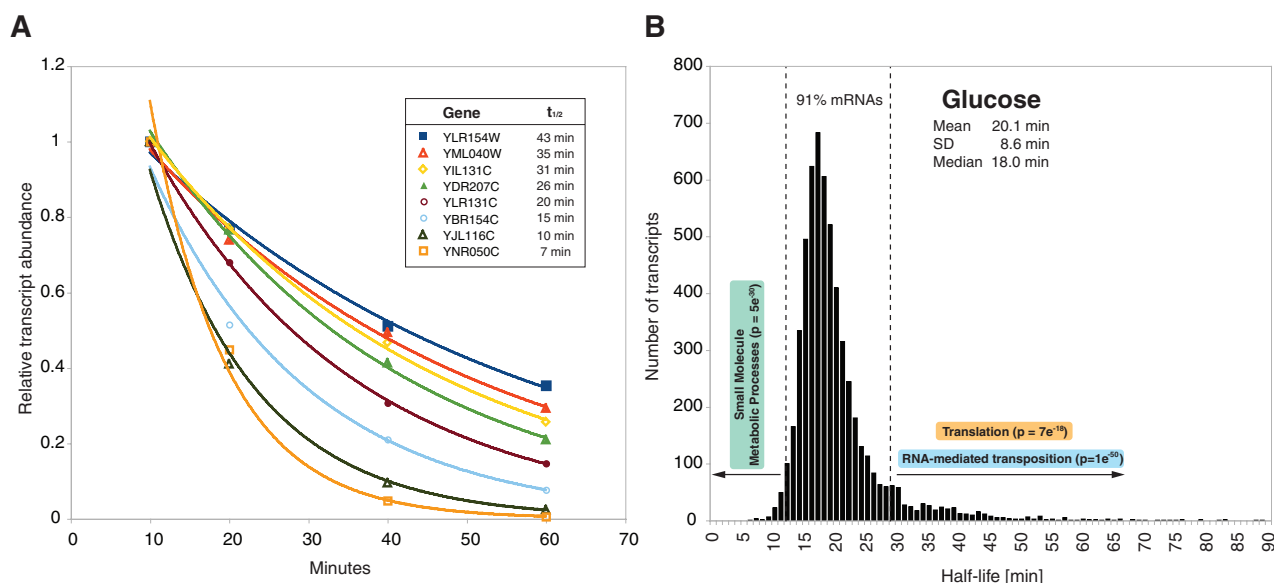

FIGURE 3: Steady-state growth analysis in glucose. (A) Individual decay curves for transcripts show a wide distribution of half-lives. Transcript abundance for each transcript was normalized to the 10-min time point. A single-exponential decay curve was fitted to all time points for each mRNA, and individual half-lives were calculated. (B) mRNA half-life distribution for cells grown in 2% glucose. Vertical lines mark approximately ±1 SD from the mean of the distribution, which contains 91% of the transcripts. Functionally related groups of mRNAs that are significantly enriched in the tails of the distribution (more than 1 SD from the mean) were identified by GO and are reported with p values. The mean, SD, and median were calculated for all genes that had a half-life between 0 and 200 min.
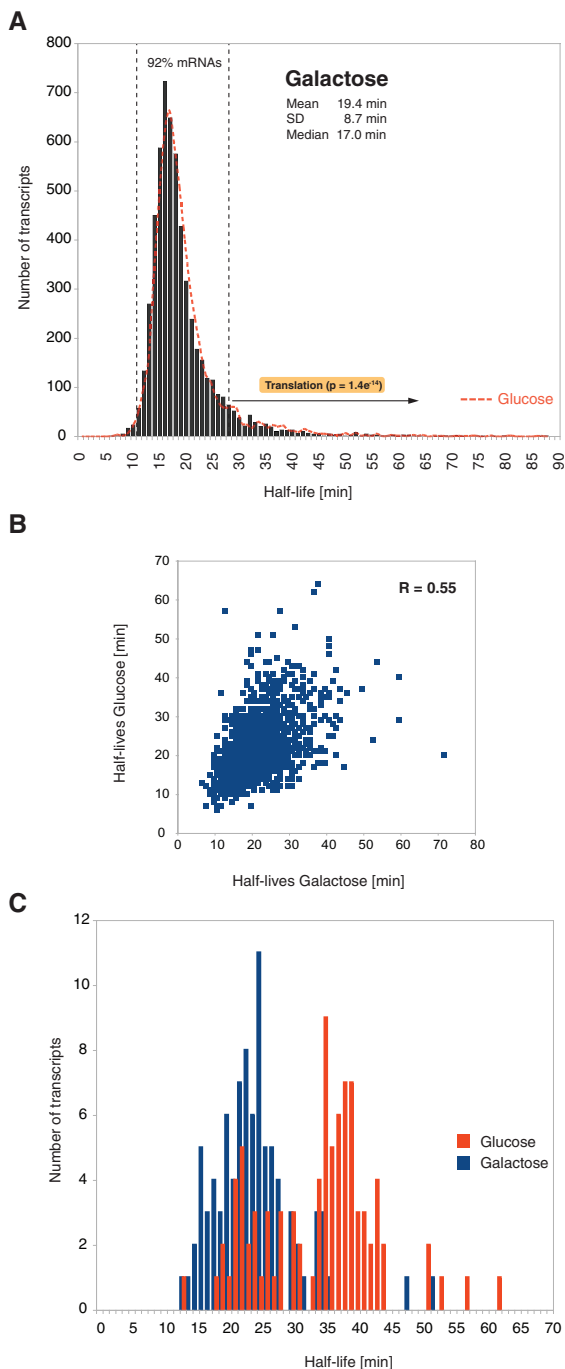
A

B

C

FIGURE 4: Steady-state growth analysis in galactose. (A) mRNA half-life distribution for cells grown in 2% galactose. Vertical lines mark approximately ±1 SD from the mean of the distribution, which contains 92% of the transcripts. The group of mRNAs functioning in translation is significantly enriched within mRNAs, which have half-lives that are longer than 1 SD from the mean. mRNA groups were identified by GO and are reported with p values. The half-life distribution for cells grown in glucose (Figure 3B) is overlaid in red for comparison. The mean, SD, and median were calculated for all genes that had a half-life between 0 and 200 min. (B) Comparison of individual mRNA half-lives for cells grown in glucose or galactose. The x- and y-axes indicate mRNA half-lives in minutes in galactose and glucose, respectively. The correlation coefficient (R) was calculated for all mRNA half-lives that have $R^2 > 0.8$ in both conditions. (C) Distributions of mRNA half-lives for transcripts involved in RNA-mediated transposition in glucose (red) vs. galactose (blue)

monitor dynamics of mRNA decay upon acute changes in growth conditions. We therefore analyzed the GAL mRNA and global turnover profile in cells shifted from galactose to glucose, representing a change to more favorable growth conditions. No drastic overall variation in global mRNA turnover rates could be observed when compared with exponential growth in glucose (mean half-life, 18.5 min; SD, 11.4; median half-life, 16 min; R = 0.41 for galactose-to-glucose shift, compared with glucose growth for mRNAs, which have $R^2 \geq 0.8$; Supplemental Figure S5). By contrast, a severe destabilization of the GAL mRNAs was observed after this transition, and their average half-life decreased from 18 to 8 min (Table 1). This mRNA half-life shortening is specific to inducible GAL mRNAs, as constitutively expressed GAL messages such as the ones encoding the transcriptional regulator Gal4 or Gal80 do not display a similar change in half-life upon a galactose-to-glucose shift.

To begin to investigate the molecular mechanism of GAL mRNA half-life regulation by glucose, we took advantage of a Gal4-VP16 fusion to the steroid hormone–binding domain of the human estrogen receptor (Gal4-ER; Louvion et al., 1993). Gal4 is the critical transcription factor regulating the transcription of all GAL genes, and expression of a Gal4-ER fusion protein enables the estrogen-dependent expression of GAL genes independent of carbon source (Louvion et al., 1993). It is intriguing that the GAL mRNAs were stable when GAL gene expression was induced via the Gal4-ER system in the presence of glucose (average $t_{1/2}$ = 24.7 min). This demonstrates that glucose per se is not sufficient to accelerate the decay of GAL mRNAs.

This result could be explained if either yeast cells have the ability to sense the acute transition from galactose to glucose or one of the Gal4-regulated gene products is required for the half-life regulation. To distinguish between these possibilities, we also analyzed the mRNA decay of GAL7 when expressed alone under the control of the constitutive ADH1 promoter in the presence of glucose. GAL7 codes for the nonregulatory galactose-1-phosphate uridyl transferase, and the endogenous GAL7 mRNA is not significantly expressed in the presence of glucose. The GAL7 mRNA half-life under the ADH1 control in glucose was nearly identical to the half-life measured during prolonged growth in galactose ($t_{1/2}$ = 15 and 16 min, respectively). Consistent with this, the GAL1, 2, 3, 5, and 10 mRNAs, which can be detected at very low levels in wild-type cells even in the presence of glucose, also displayed long half-lives (Table 1). Thus, it is not the presence of glucose alone that is responsible for the changes in half-life, but instead yeast respond to the acute change in carbon source from galactose to glucose to dramatically shorten the half-lives of the GAL mRNAs. This suggests the existence of a coupling mechanism between transcriptional inhibition in the nucleus and enhanced decay in the cytoplasm, which in combination allows yeast cells to rapidly turn off the expression of the GAL genes upon return to glucose. It will now be interesting to dissect the signaling pathway and the molecular mechanism that leads to the rapid decay of the GAL mRNAs upon addition of glucose.

Monitoring mRNA turnover upon glucose starvation

We next applied our metabolic labeling protocol to profile mRNA decay during cellular stress. Yeast cells respond to acute glucose starvation with a number of well-characterized transcriptional and physiological changes (Zaman et al., 2008). Hence we analyzed the changes in mRNA turnover that occur when cells were starved for glucose, by switching the carbon source from glucose to galactose at the beginning of the chase period. In contrast to the limited global changes that could be detected in the growth
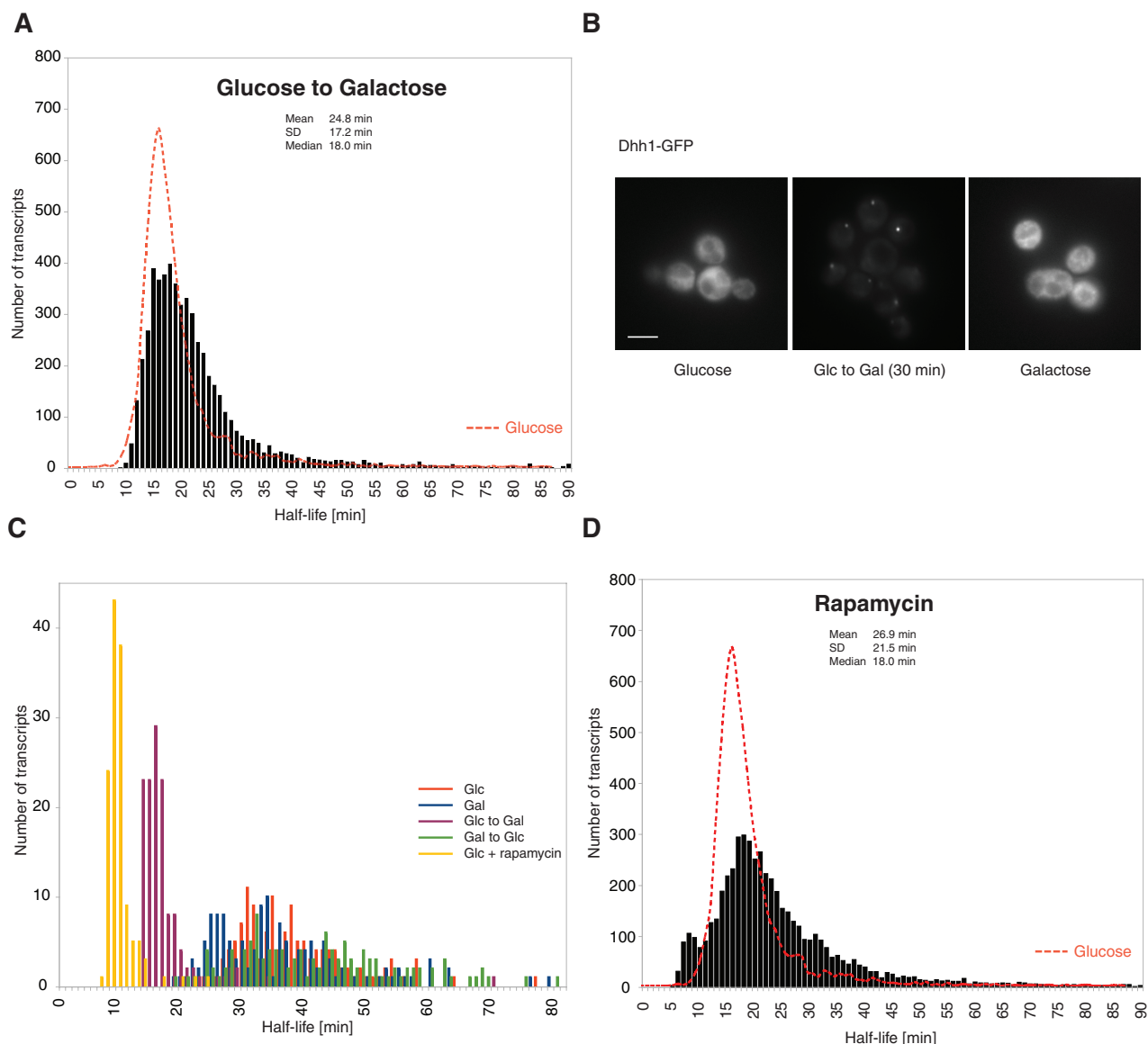
FIGURE 5: Acute perturbations. (A) Half-life distribution for cells upon acute shift from 2% glucose into 2% galactose. For comparison, the half-life distribution for cells grown in glucose (Figure 3B) is overlaid in red. (B) In vivo localization of Dhh1-GFP, a P-body marker, in 2% glucose (left), 30 min following shift from 2% glucose to 2% galactose (middle), and in 2% galactose (right). Bar, 5 μm. (C) mRNA half-life distributions for transcripts involved in translation in glucose (red), galactose (blue), glucose-to-galactose shift (purple), galactose-to-glucose shift (green), and upon rapamycin treatment in glucose (yellow). (D) Distribution of mRNA half-lives for cells treated with rapamycin. The mean, SD, and median were calculated for all genes that had a half-life between 0 and 200 min. For comparison, the half-life distribution for cells grown in glucose (Figure 3B) is overlaid in red.

conditions analyzed so far, we observed a significant overall stabilization of mRNAs in response to this carbon source change. The average mRNA half-life shifted from 20.1 min in glucose to 24.8 min during the glucose-to-galactose transition, with 56% of all mRNAs showing a significantly longer half-life. Furthermore, the distribution of half-lives widened considerably, and the SD of the half-life distribution doubled from 8.6 min in glucose to 17.2 min in the glucose-to-galactose shift (Figure 5A; R = 0.2 for glucose-to-galactose shift, compared with glucose growth for mRNAs, which have an $R^2 \geq 0.8$). The observed global stabilization correlates with a halt in cellular growth and the formation of P bodies (Figure 5B) implicated in mRNA storage and decay (Balagopal and Parker, 2009).

Although the majority of mRNAs were stabilized upon glucose-to-galactose shift, the opposite consequence was observed for mRNAs coding for ribosomal proteins. During growth in glucose, these mRNAs were exceptionally stable (Figure 3B), but upon shift into galactose medium, 132 of 132 detected ribosomal protein mRNAs exhibited an increase in their decay rates. Their average half-life was reduced from 38 to 16.4 min (Figure 5C), and ribosome biogenesis genes were highly enriched among transcripts, with a half-life of 12 min or less ($p = 1.4e^{-45}$). Of interest, addition of galactose and concomitant withdrawal of glucose was previously shown to inhibit growth, translation, and new ribosome biosynthesis at the level of transcription (Warner, 1999; Zaman et al., 2008). Here, we show in addition that yeast cells increase the degradation of

	GAL1	GAL2	GAL3	GAL5/PGM2	GAL7/ADH1:GAL7	GAL10
Galactose	17	21	21	15	16/–	20
Glucose + Gal4-ER	22	34	18	34	18/–	22
Galactose to glucose	5	9	11	10	6/–	7
Glucose	19	21	16	16	–/15	20

TABLE 1: Measured half-lives (minutes) of genes involved in galactose metabolism under various growth conditions.

ribosomal protein mRNAs during this carbon source stress. Furthermore, we demonstrate that this is accompanied by a global stabilization of mRNAs. These dramatic changes in mRNA turnover presumably help yeast cells to respond to carbon source stress by storing bulk mRNAs and simultaneously reducing new protein synthesis by rapidly degrading mRNAs that would produce new ribosomal proteins. However, these changes in mRNA decay are temporary, and yeast cells adapt. On extended growth in galactose, the regular turnover profile is restored (Figure 4A), P-bodies disappear (Figure 5B), and ribosomal protein mRNAs are stabilized (Figure 5C).

Effects of target of rapamycin signaling on mRNA turnover

A critical regulator of growth in response to nutrient availability is the highly conserved target-of-rapamycin (TOR) signaling pathway. In yeast, inhibition of TOR signaling induces growth arrest and causes a general down-regulation of protein synthesis at the level of both translation and ribosome biogenesis (De Virgilio and Loewith, 2006; Wullschleger et al., 2006). Furthermore, TOR signaling was previously shown to affect the turnover of a subset of mRNAs (Albig and Decker, 2001). To test whether down-regulation of the TOR pathway affects global mRNA turnover, cells grown in glucose were treated with the TOR kinase inhibitor rapamycin (Brown et al., 1994) and mRNA decay profiles were analyzed (Figure 5D). As in the glucose-to-galactose shift, rapamycin induced a global mRNA stabilization and widened the distribution of the overall decay profile (the average half-life increased from 20.1 to 26.9 min and the SD increased from 8.6 to 21.5 min, respectively). Furthermore, the glucose-to-galactose and rapamycin data sets were positively correlated (R = 0.45). Both TOR pathway inhibition and acute glucose starvation (e.g., when the carbon source is changed to galactose) lead to a global inhibition of translation indicating a link between translational activity and mRNA turnover. It is intriguing that rapamycin treatment also dramatically shortened the average half-life of all 132 detected ribosomal protein mRNAs to 8.96 min. Again, ribosome biogenesis genes were highly enriched in transcripts with a half-life of 12 min or less (p = 2.72e^{-157}; Figure 5C). This suggests that active TOR signaling is required for the extended half-life of ribosomal protein mRNAs observed in logarithmically growing cells. Thus, the TOR pathway may coordinate cell division and growth with protein synthesis, mRNA storage, and decay.

In this study, we measured mRNA decay rates at a system-wide level in budding yeast in multiple growth conditions. Our analyses discovered cellular programs that coordinate mRNA turnover rates for functionally related mRNAs or for the bulk mRNA population. The mechanistic details of how these gene-specific and global changes are mediated can now be investigated. Furthermore, our results have identified the TOR signaling pathway as an important regulator of mRNA decay, implicating TOR as a key regulator of gene expression in response to nutrient stress by integrating changes in mRNA turnover with changes in transcription and translation. It will be of interest to dissect these newly identified regulatory

programs and to characterize potential cis- and trans-acting factors that regulate these changes in RNA half-life. Although we focused here on the analysis of mRNA turnover, our metabolic labeling protocol can also be modified to directly measure transcription rates in actively growing cells. Thus, this approach provides a powerful tool to dissect the kinetics of both mRNA decay and transcription and will help to characterize the complex changes in mRNA abundance that occur in cells during various growth conditions or during development.

MATERIALS AND METHODS
Strains

All strains used were derivatives of S. cerevisiae W303-1A {MATa, leu2-3112 trp1-1 can1-100 ura3-1 ade2-1 his3-11,15}. To generate a strain expressing GAL7 under the control of the ADH1 promoter, the ADH1 promoter and GAL7 open reading frame including the 5′ and 3′ UTRs were cloned into pRS403 (via HindIII/EcoRI and BamHI/XbaI, respectively) to generate pKW2539. On digestion with Nhe1, pKW2539 was transformed into W303. The correct insertion of the ADH1-GAL7 fragment into the HIS3 locus was confirmed by PCR.

Pulse-chase conditions

Yeast were grown to midlog phase at 30°C in synthetic drop-out media (0.67% yeast nitrogen base without amino acids), 2% appropriate sugar, and with all amino acids supplemented at established concentrations, except uracil, which was present at 0.1 mM. For pulse, a final concentration of 0.2 mM 4TU was added to log-phase yeast cultures grown for 3 h. Yeast were spun down at 3000 rpm for 2 min and resuspended in drop-out media containing 20 mM uracil (chase). Yeast samples were collected immediately by filtration over a 0.8 micron nitrocellulose membrane (Millipore, Billerica, MA) at the following time points: t = 0, 5, 10, 20, 30, 45, 60, and 90 min. Collected samples were normalized to 1 × 10^8 cells per time point and immediately frozen in liquid nitrogen.

RNA preparation, biotinylation, and purification

Total RNA was isolated using RiboPure RNA Isolation kit (Ambion, Austin, TX). One hundred μg of total RNA was biotinylated as previously described using EZ-Link Biotin-HPDP (Pierce, Thermo Fisher Scientific, Rockford, IL; Zeiner et al., 2008). Oligo(dT) purifications were performed using oligo(dT)$_{25}$ Dynabeads and established manufacturer protocols (Invitrogen, Carlsbad, CA).

Purification of biotinylated RNAs was carried out using magnetic MyOne Streptavidin beads (Invitrogen) and the protocol adapted from previous studies (Zeiner et al., 2008). One microliter of beads was used per 160 ng of mRNA, with the minimum volume of beads being 25 μl. Biotinylated RNAs were incubated with beads in 0.75 M NaCl, 10 mM EDTA, and 10 mM Tris-Cl, pH 7.4, for 10 min at 22°C. RNA was eluted by resuspending the beads in 1× volume of a 5% β-mercaptoethanol (BME) solution and incubating at 22°C for 5 min.

Two rounds of BME elution were performed. The eluates were combined, and 20 µg of linear acrylamide (Ambion) was added as a carrier. RNA was precipitated using isopropanol and NaCl (as described earlier) and resuspended in 10 µl of water.

cDNA library synthesis

Purified mRNA samples were fragmented using Fragmentation Buffer (AM8740) from Ambion at 70°C for 5 min. Fragmented mRNA was precipitated using 0.1× volume of 5 M NaCl and 3× volume of 100% ethanol and incubated at −80°C for 30 min. mRNA samples were then resuspended in 10.5 µl of water.

For first-strand cDNA synthesis, ~200 ng of mRNA was mixed with 3 µg of random hexamer primers, incubated at 65°C for 5 min, and then immediately placed on ice. cDNA synthesis was carried out using Superscript II reverse transcriptase according to the manufacturer's protocol (Invitrogen). Next, second-strand synthesis buffer was added (50 mM Tris-HCl, pH 7.8, 5 mM $MgCl_2$, and 1 mM dithiothreitol) in addition to *Escherichia coli* polymerase I, dNTPS, and RNAse H to nick translate the second-strand synthesis for 2.5 h at 16°C. The reaction was then cleaned up on a QiaQuick PCR column and eluted in 30 µl of EB buffer (Qiagen, Valencia, CA).

Library preparation and normalization for Illumina sequencing

The Illumina (San Diego, CA) library was prepared according to the manufacturer's instructions with a 200–base pair size selection (http://www.illumina.com). Libraries were sequenced as single 32-mer reads using the standard Solexa pipeline.

For normalization between time points, an in vitro–transcribed RNA was spiked into samples for each time point to serve as an internal standard. Human importin alpha (hSRP1alpha) was cloned into pBluescript vector containing a T3 promoter and polyA tail, then linearized to give transcripts of 1500–base pair length. In vitro transcription reactions were labeled with 4-thio-UTP (Jena Bioscience, Jena, Germany) at a ratio of one part UTP to two parts label using Ambion MegaScript Kit (Ambion). Six ng of transcribed RNA standard was spiked into 100 µg of total RNA prior to biotinylation reactions and carried throughout all purifications and sequencing reactions. This constant amount of RNA was used to normalize the sequencing results from each time point to a constant, allowing for comparison across the time course.

Data analysis

The Solexa reads were aligned to all yeast open reading frames, including introns, as annotated in "orf_genomic.fasta" (http://www.yeastgenome.org/), using the program Bowtie (Langmead *et al.*, 2009). The number of reads was uniformly normalized at each time point so that the number of the spiked-in hSRP1alpha reads was constant across all time points. The equation for a single-exponential decay curve is

$$A=A_0 e^{-k_{decay} t}$$

where A is the number of molecules at some time t, given the number of molecules at 0 min (A_0) and the decay constant k_{decay}. A single-exponential curve was fitted to the reads for all time points between 10 and 60 min by calculating the k_{decay} that gave the greatest nonlinear regression value between the measured data and a theoretical decay curve using the program Calc (http://www.openoffice.org/). The half-life for each gene was calculated using the equation

$$t_{1/2} = \ln(2)/(k_{decay} - K_{growth})$$

where k_{growth} is the measured rate of growth of the culture during the course the experiment. Subtraction of k_{growth} is necessary to account for the dilution of the labeled mRNAs by newly synthesized transcripts in the population post pulse. Functionally related genes that had significantly similar half-lives were identified in the tails of the half-life distribution (more than one SD from the mean; see Figure 2) by the yeast Gene Ontology (GO) server with default parameters (http://www.yeastgenome.org/).

A half-life curve generator program was developed and used to automate the display of mRNA decay curves and half-life distributions in all conditions tested. The program is available at http://rnadecay.berkeley.edu/.

REFERENCES

Albig AR, Decker CJ (2001). The target of rapamycin signaling pathway regulates mRNA turnover in the yeast *Saccharomyces cerevisiae*. Mol Biol Cell 12, 3428–3438.

Balagopal V, Parker R (2009). Polysomes, P bodies and stress granules: states and fates of eukaryotic mRNAs. Curr Opin Cell Biol 21, 403–408.

Bennett MR, Pang WL, Ostroff NA, Baumgartner BL, Nayak S, Tsimring LS, Hasty J (2008). Metabolic gene regulation in a dynamically changing environment. Nature 454, 1119–1122.

Boeke JD, Garfinkel DJ, Styles CA, Fink GR (1985). Ty elements transpose through an RNA intermediate. Cell 40, 491–500.

Brown EJ, Albers MW, Shin TB, Ichikawa K, Keith CT, Lane WS, Schreiber SL (1994). A mammalian protein targeted by G1-arresting rapamycin-receptor complex. Nature 369, 756–758.

Cheadle C, Fan J, Cho-Chung YS, Werner T, Ray J, Do L, Gorospe M, Becker KG (2005). Stability regulation of mRNA and the control of gene expression. Ann NY Acad Sci 1058, 196–204.

Checkley MA, Nagashima K, Lockett SJ, Nyswaner KM, Garfinkel DJ (2010). P-body components are required for Ty1 retrotransposition during assembly of retrotransposition-competent virus-like particles. Mol Cell Biol 30, 382–398.

Cleary MD, Meiering CD, Jan E, Guymon R, Boothroyd JC (2005). Biosynthetic labeling of RNA with uracil phosphoribosyltransferase allows cell-specific microarray analysis of mRNA synthesis and decay. Nat Biotechnol 23, 232–237.

Coller J, Parker R (2004). Eukaryotic mRNA decapping. Annu Rev Biochem 73, 861–890.

De Virgilio C, Loewith R (2006). The TOR signalling network from yeast to man. Int J Biochem Cell Biol 38, 1476–1481.

Dutko JA, Kenny AE, Gamache ER, Curcio MJ (2010). 5′ to 3′ mRNA decay factors colocalize with Ty1 gag and human APOBEC3G and promote Ty1 retrotransposition. J Virol 84, 5052–5066.

Eulalio A, Behm-Ansmant I, Izaurralde E (2007). P bodies: at the crossroads of post-transcriptional pathways. Nat Rev Mol Cell Biol 8, 9–22.

Franks TM, Lykke-Andersen J (2008). The control of mRNA decapping and P-body formation. Mol Cell 32, 605–615.

Garneau NL, Wilusz J, Wilusz CJ (2007). The highways and byways of mRNA decay. Nat Rev Mol Cell Biol 8, 113–126.

Grigull J, Mnaimneh S, Pootoolal J, Robinson MD, Hughes TR (2004). Genome-wide analysis of mRNA stability using transcription inhibitors and microarrays reveals posttranscriptional control of ribosome biogenesis factors. Mol Cell Biol 24, 5534–5547.

Langmead B, Trapnell C, Pop M, Salzberg SL (2009). Ultrafast and memory-efficient alignment of short DNA sequences to the human genome. Genome Biol 10, R25.

Lohr D, Venkov P, Zlatanova J (1995). Transcriptional regulation in the yeast GAL gene family: a complex genetic network. FASEB J 9, 777–787.

Louvion JF, Havaux-Copf B, Picard D (1993). Fusion of GAL4-VP16 to a steroid-binding domain provides a tool for gratuitous induction of galactose-responsive genes in yeast. Gene 131, 129–134.

Parker R, Sheth U (2007). P bodies and the control of mRNA translation and degradation. Mol Cell 25, 635–646.

Pelechano V, Perez-Ortin J (2008). The transcriptional inhibitor thiolutin blocks mRNA degradation in yeast. Yeast 25, 85–92.

Sharova LV, Sharov AA, Nedorezov T, Piao Y, Shaik N, Ko MS (2009). Database for mRNA half-life of 19 977 genes obtained by DNA microarray analysis of pluripotent and differentiating mouse embryonic stem cells. DNA Res 16, 45–58.

Wang Y, Liu CL, Storey JD, Tibshirani RJ, Herschlag D, Brown PO (2002). Precision and functional specificity in mRNA decay. Proc Natl Acad Sci USA 99, 5860–5865.

Wang Z, Gerstein M, Snyder M (2009). RNA-Seq: a revolutionary tool for transcriptomics. Nat Rev Genet 10, 57–63.

Warner JR (1999). The economics of ribosome biosynthesis in yeast. Trends Biochem Sci 24, 437–440.

Wilhelm BT, Landry JR (2009). RNA-Seq-quantitative measurement of expression through massively parallel RNA-sequencing. Methods 48, 249–257.

Wullschleger S, Loewith R, Hall MN (2006). TOR signaling in growth and metabolism. Cell 124, 471–484.

Zaman S, Lippman SI, Zhao X, Broach JR (2008). How Saccharomyces responds to nutrients. Annu Rev Genet 42, 27–81.

Zeiner GM, Cleary MD, Fouts AE, Meiring CD, Mocarski ES, Boothroyd JC (2008). RNA analysis by biosynthetic tagging using 4-thiouracil and uracil phosphoribosyltransferase. Methods Mol Biol 419, 135–146.